

## **IN-SITU WATER UPTAKE RATE MEASUREMENT OF AQSOA FAM-Z02 PACKED IN FINNED TUBE ADSORBER BEDS OF AN ADSORPTION COOLING SYSTEM**

**Seyyed Mahdi Nemati Mehr, Amir Sharafian, Wendell Huttema, Majid Bahrani**

Laboratory for Alternative Energy Conversion (LAEC)  
School of Mechatronic Systems Engineering  
Simon Fraser University  
#4300, 250-13450 102 Avenue, Surrey, BC, Canada V3T0A3  
Tel: +1 (778) 782-8538; E-mail: mbahrani@sfu.ca

### **Abstract**

Adsorption cooling systems (ACS) utilize waste heat or low-grade thermal energy to produce the cooling power required for air conditioning and refrigeration (A/C-R) in buildings and mobile applications. However, the bulkiness and heavy weight of ACS presently limit its commercialization. To minimize the footprint of ACS, different materials with high uptake rate have been developed. Thermogravimetric analysis (TGA) is a well-known technique for measuring the adsorbate uptake rate of an adsorbent material. However, this method does not consider the effects of adsorber bed geometry, interparticle mass transfer resistances, and pressure drop. In a real ACS, adsorbent material is packed in an adsorber bed protected with metallic wire mesh. These geometrical constraints may limit the uptake rate of the adsorbent material. In this study, the water uptake rate of AQSOA FAM-Z02 packed in an adsorber bed was measured in-situ under the adsorption temperature of 30°C and desorption temperature of 90°C while the water source temperature was held constant at 20°C. Two different heat exchanger designs were chosen and the water uptake rate was measured by monitoring the heat exchanger's mass in real time. The results show that the adsorber with higher surface area and 10 fins per inch (FPI) provides the specific cooling power (SCP) of as high as 110 W/kg at cycle time of 8 min and three times higher SCP than the adsorbed bed with 3 FPI under cycle time of 60 min.

### **KEYWORDS**

In-situ mass measurement, FAM-Z02, adsorber bed, adsorption cooling system.

### **INTRODUCTION**

Air conditioning and refrigeration (A/C-R) systems are responsible for using about 30% of total worldwide energy [1] and the number of A/C-R units is expected to reach 78.8 million by 2015. The Supplemental Federate Test Procedure (SFTP) for emission test of A/C systems (SC03) in vehicles with gross weight of under 2608 kg (5750 lb) showed that A/C systems contribute to 37% of the total tailpipe emissions [2]. Furthermore, about 70% of total fuel energy released in an internal combustion engine (ICE) is wasted as heat that is dissipated through the engine coolant and exhaust gas [3]. To reduce the environmental impacts of A/C systems and reduce fuel consumption in mobile applications, waste heat-driven adsorption cooling systems (ACSs) are potential energy efficient replacements for vapor compression refrigeration cycles (VCRC) where low-grade thermal energy is available. An ACS can use the waste heat of an ICE to provide cooling in vehicles and drastically reduce vehicles' fuel consumption and carbon-footprint.

A waste heat-driven ACS uses an adsorbate, such as water or methanol, which is adsorbed and desorbed from the surface of an adsorbent, such as zeolite, silica gel, or activated carbon. Most of these materials are non-toxic, non-corrosive, and inexpensive [4] making ACS a safe and environmentally friendly technology. An ACS operates more quietly than a VCRC and is easier to maintain because its only moving parts are valves [5]. However, current ACS are limited in their usefulness for commercial vehicle applications, specifically light-duty vehicles, because of their bulkiness and heavy weight. These properties result in a low coefficient of performance ( $COP = \text{cooling energy} / \text{input energy}$ ) and low specific cooling power ( $SCP = \text{cooling energy} / (\text{adsorbent mass} \times \text{cycle time})$ ). The origins of the low COP and SCP are the low thermal conductivity of adsorbent particles ( $\sim 0.1$  to  $0.4 \text{ W}/(\text{m}\cdot\text{K})$ ) [6–8] and low mass diffusivity of adsorbent-adsorbate pairs ( $\sim 10^{-8}$  to  $10^{-14} \text{ m}^2/\text{s}$ ) [7,9].

To overcome these limitations, different adsorbent materials with high thermal conductivity and high adsorbate uptake have been developed such as the ones reported in Ref. [10,11]. AQSOA FAM-Z02 is one of these synthesized materials developed for A/C applications by Mitsubishi Chemical Ltd. [12]. FAM-Z02 showed high durability of 60,000 cycles and low desorption temperature of 75-95°C [12] making it a good candidate for mobile applications. Thermogravimetric analysis (TGA) is a well-known technique to measure the adsorbate uptake of FAM-Z02. In A TGA, mass changes of a few milligrams of the adsorbent during an adsorption/desorption process are measured versus time under a controlled temperature and pressure. This information for FAM-Z02 can be found in Ref. [13,14]. In real applications, however, effects of ACS adsorber bed geometry, interparticle mass transfer resistances, and pressure drop as well as the effects of other component of ACS, e.g. condenser and evaporator, may reduce the performance of ACS. Therefore, these geometrical constraints limit the uptake rate of adsorbent material, e.g., FAM-Z02, within the short periods of adsorption and desorption.

In this study, the water uptake rate of FAM-Z02 packed in two different adsorber beds is measured in-situ under the adsorption and desorption temperatures of 30°C and 90°C while the water source temperature is kept at 20°C. Finally, the SCP of ACS is reported under different cycle times.

## EXPERIMENTAL TESTBED

To measure the mass exchange of an adsorbent packed in an adsorber bed during the adsorption and desorption processes, a setup was designed and built as shown in

Fig. 1. The adsorber bed was placed on a scale (Setra, Supper II) with  $\pm 1$  g accuracy and connected to heating and cooling fluid temperature control systems,  $TCS_{HF}$  and  $TCS_{CF}$ , for intermittent desorption and adsorption. A water source at a constant temperature, as shown in

Fig. 1, was connected to the adsorber bed using a vacuum rated flexible hose. This water source served as an evaporator or a condenser during the adsorption and desorption processes, respectively.

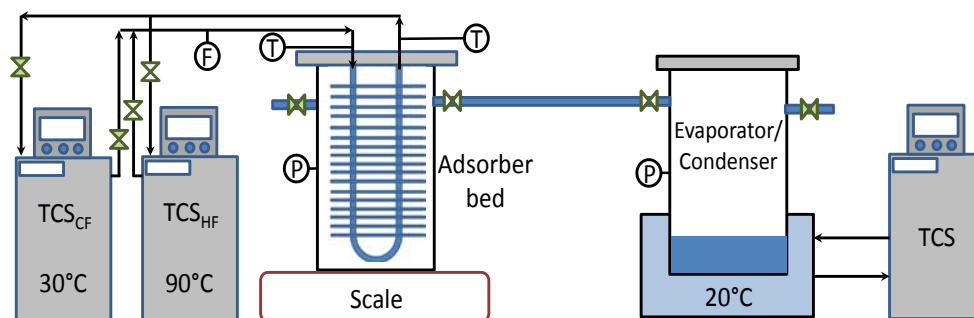


Fig. 1. Schematic of the experimental test setup.

As shown in Fig.2, two heat exchangers with different geometries (#1 in Fig.2) were tested while they were connected to a controlled temperature water source (# 3 in Fig.2). The first heat exchanger (called Design I) was built based on the results of Sharafian et al. [15] and was placed inside a vacuum chamber, as shown in Fig.2a. The second adsorber bed (called Design II) which was an engine oil cooler manufactured by Hayden Automotive (model #1268) was placed in a custom-built vacuum chamber, as shown in Fig.2b. The heat exchangers in Designs I and II had 3 and 10 fins per inch (FPI), respectively. To measure the temperature and pressure of the adsorber beds and evaporator, and heating and cooling fluid flow rates, thermocouples type T (Omega, model #5SRTC-TT-T-36-36) with accuracy of  $\pm 0.1^\circ\text{C}$ , a pressure transducer with 0-34.5 kPa operating range (Omega, model #PX309-005AI) and  $\pm 0.4$  kPa accuracy, and a positive displacement flow meter (FLOMEC, Model # OM015S001-222) with accuracy of 0.5% of reading were installed on the systems. Further details on the adsorber beds and operating conditions are summarized in Table 1.

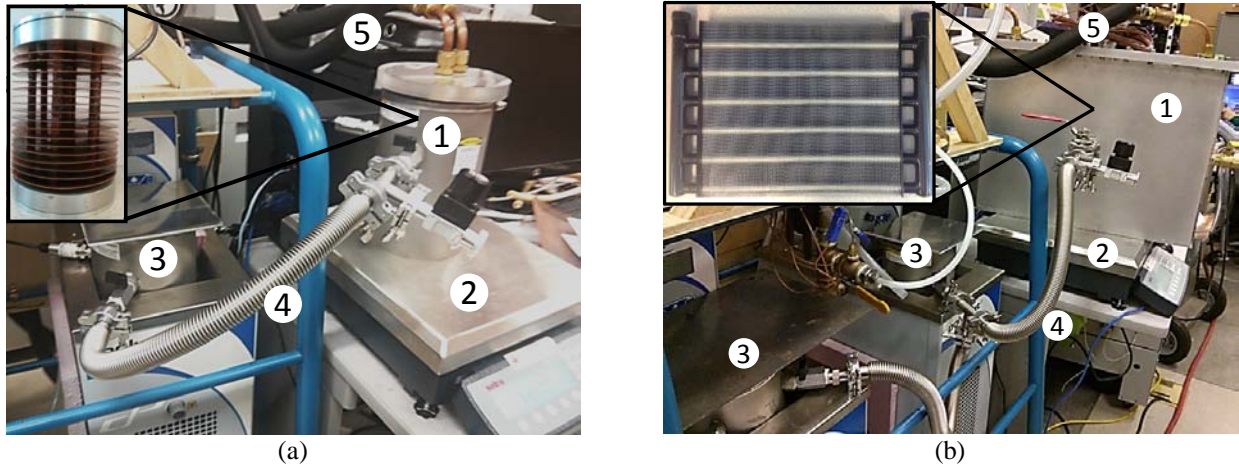


Fig.2. Details of the experimental setup for (a) Design I and (b) Design II. 1: adsorber bed, 2: scale, 3: evaporator, 4: flexible hose, and 5: heating/cooling fluid ports.

Table 1. Operating conditions for the experiments.

Parameter	Design I	Design II
Working pairs	AQSOA FAM-Z02/water	
Adsorbent particles diameter (m)	0.002	
Mass of adsorbent (kg)	0.62	1.50
Metal mass of adsorber bed (kg)	2.80	2.87
Adsorber bed heat transfer surface area, $A_{bed}$ , (m <sup>2</sup> )	0.235	2.80
Number of fins per inch (FPI)	3	10
Fin dimensions	12.7 cm (5") diameter	43.18×30.48 cm (17"×12")
Heating fluid mass flow rate to adsorber bed (kg/s)	0.058 (4.1 L/min of silicone oil)	
Cooling fluid mass flow rate to adsorber bed (kg/s)	0.062 (4.1 L/min of silicone oil)	
Heat capacity of silicone oil (kJ/kgK)	1.8	
Heating fluid inlet temperature (°C)	90	
Cooling fluid inlet temperature (°C)	30	
Evaporation/condensation temperature (°C)	20	

As shown in Table 1, the amount of adsorbent material inside the adsorber bed of Design II is more than that of Design I. To supply enough vapor during adsorption process, two evaporator of the same type was connected to the adsorber bed of Design II, as shown in Fig.2b. To run a set of measurements, the adsorber bed packed with FAM-Z02 was heated using a 90°C heating fluid and simultaneously evacuated for 8 hours to be completely dire out. The adsorber bed was placed on the scale and was connected to the evaporator. By opening the valve between the adsorber bed and evaporator, the mass change of the adsorber bed during adsorption and desorption processes was measured versus time.

To heat up and cool down the adsorber bed, a silicone oil heating fluid (Julabo, Thermal P60) was used. Due to the temperature difference between the heating and cooling fluids (90°C and 30°C), the silicone oil density was changed. To precisely measure the water uptake rate of FAM-Z02, the density change of the silicone oil should be de-convoluted from the mass change measured. To this end, the mass change of the adsorber bed was measured separately when it was not connected to the evaporator.

## DATA ANALYSIS

To evaluate the performance of adsorber beds, the SCP of the ACS should be calculated. Equation (1) gives the ideal evaporation cooling energy calculated based on the in-situ water uptake rate measurement of FAM-Z02:

$$Q_{evap,ideal} (J) = \Delta\omega_{adsorption} m_{adsorbent} h_{fg} \quad (1)$$

where  $\Delta\omega_{adsorption}$  is equal to  $\Delta m_{adsorbate\ update}/m_{adsorbent}$ , i.e. the amount of water adsorbed during the adsorption process per mass of dry adsorbent, and  $h_{fg}$  is the enthalpy of evaporation of water at the evaporator temperature. In this study, the ideal evaporation cooling effect refers to an evaporator with the effectiveness of one and thermal mass of zero in which there is no temperature drop between the refrigerant and the chilled water circulated inside the evaporator. This assumption is in agreement with the data measured using the TGA such as the ones reported in Ref. [14]. Using Eq.(1), the ideal SCP of the ACS are calculated as:

$$SCP_{ideal} (W / kg) = \frac{Q_{evap,ideal}}{m_{adsorbent} \tau_{cycle}} \quad (2)$$

where  $\tau_{cycle}$  is the cycle time.

## RESULTS AND DISCUSSION

Fig. 3 shows the variations in heating and cooling fluid inlet and outlet temperatures, and the mass change of the adsorber beds in Designs I and II during adsorption and desorption at cycle time of 60 min.

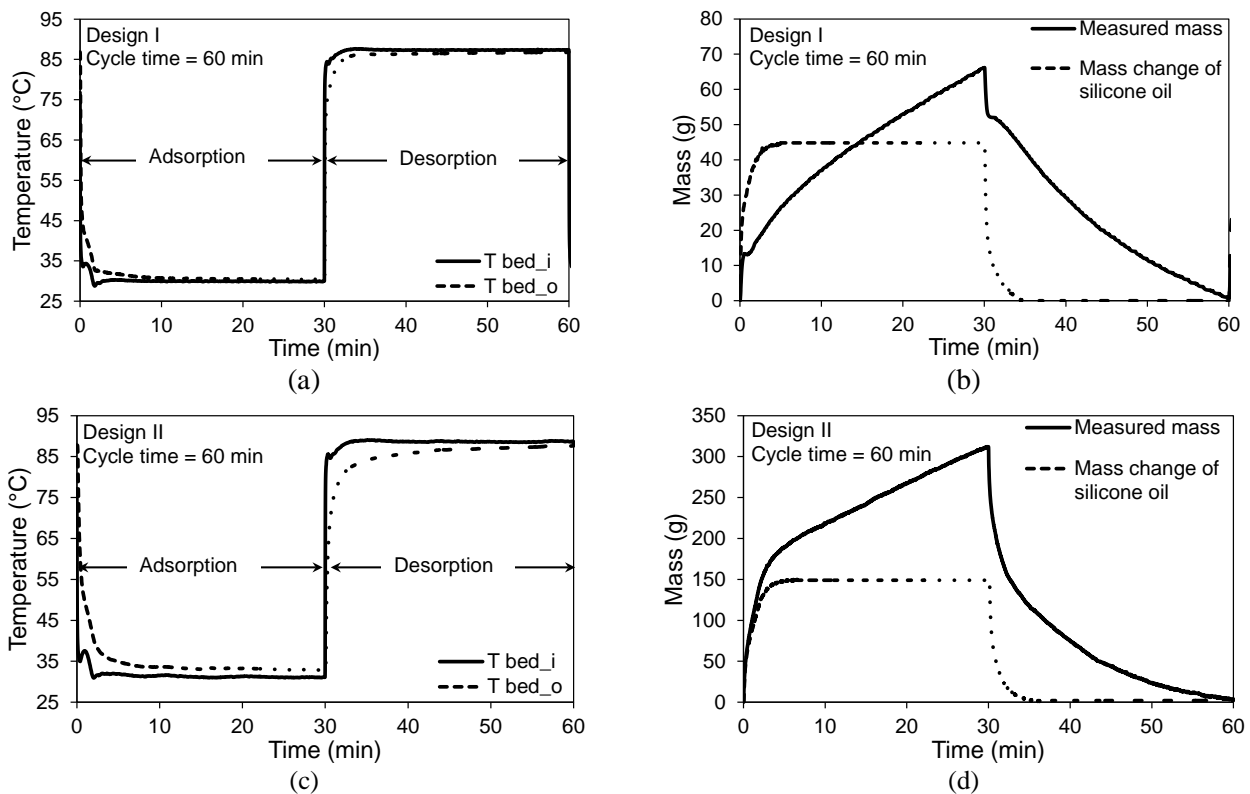


Fig. 3. Heating and cooling fluid inlet and outlet temperatures and mass change of adsorber bed and silicone oil during adsorption and desorption under cycle time of 60 min in (a)-(b) Design I and (c)-(d) Design II.

It can be seen that the adsorber bed mass, shown in Fig. 3b and Fig. 3d, increases and decreases as the adsorbent is adsorbed and desorbed. The heat transfer fluid used for heating and cooling of the adsorber beds was silicone oil that has a density change from  $909 \text{ kg/m}^3$  at  $30^\circ\text{C}$  to  $854 \text{ kg/m}^3$  (6.5%) at  $90^\circ\text{C}$ . The stiffness of flexible hosing connected to the adsorber beds also changed during heating and cooling process. To this end, the adsorber beds were disconnected from the evaporator, and heating and cooling processes were performed to measure the adsorber bed mass change caused only by the variation of heat transfer fluid

density and flexible hosing stiffness. Fig. 3b and Fig. 3c indicate that these phenomena have significant effect on the adsorber bed mass measurement.

Comparing Fig. 3a and Fig. 3c also demonstrates that the adsorber bed inlet and outlet temperature difference in Design II is more than that in Design I because of the larger heat transfer surface area and smaller fin spacing. This temperature difference shows that the adsorber bed in Design II adsorbs/desorbs more adsorbate than that in Design I within a constant cycle time. Fig. 4 shows the pressure of the evaporator/condenser chamber,  $P_{\text{evap/cond}}$ , in Designs I and II under the cycle time of 60 min. The red line in Fig. 4 shows the saturation pressure of water at 20°C (evaporator/condenser temperature). It can be seen that during adsorption, the adsorber beds create suction, evaporation happens inside the evaporator, and  $P_{\text{evap/cond}}$  reduces. Fig. 4 also shows that  $P_{\text{evap/cond}}$  is lower when the evaporator is connected to the adsorber bed in Design II than that in Design I because of higher suction created by the adsorber bed. Higher suction is a result of more adsorbate uptake by the adsorbent material.

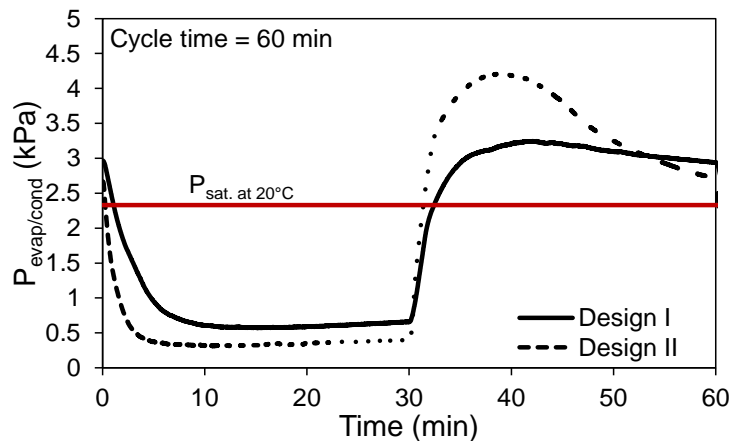


Fig. 4. Comparison of  $P_{\text{evap/cond}}$  in Designs I and II during adsorption and desorption under cycle time of 60 min. The red line demarcates the saturation pressure of water at 20°C, as shown in Table 1.

Fig. 5a shows the in-situ water uptake difference measurement for FAM-ZO2 during adsorption and desorption in Designs I and II. As shown in Fig. 5a, the adsorber bed in Design II has higher water uptake difference than that in Design I. For example, under cycle time of 60 min, the adsorber bed in Design II has uptake difference of 10.8% while that in Design I has water uptake difference of 3.5%. Also, Fig. 5 indicates that the adsorber bed in Design II can operate in shorter cycle times (8-20 min) which are of interest for mobile applications.

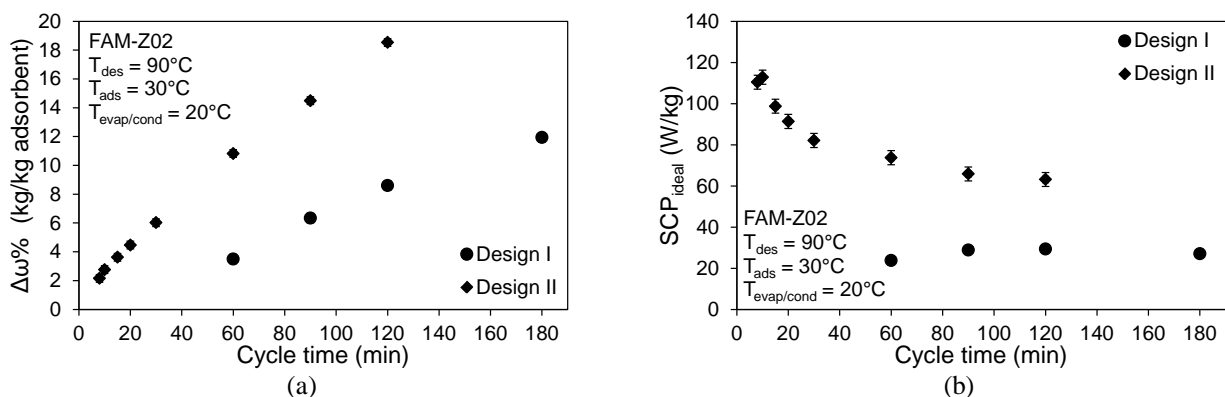


Fig. 5. (a) In-situ water uptake difference measurement of adsorber beds in Designs I and II, and (b) ideal SCP of the ACS vs. cycle time.

The SCP of ACS corresponding to the water uptake difference measurements is shown in Fig. 5b. It can be seen that the adsorber bed in Design II provides ideal SCP of 110 W/kg at cycle time of 8 min. Also,

Fig. 5b shows that under a cycle time of 60 min, Design I has SCP of 24 W/kg which is three times less than that of Design II. Finally, it can be concluded from Fig. 5 that the adsorber bed in Design II provides higher uptake and SCP.

## CONCLUSION

In this study, an experimental setup was designed to test the adsorbate uptake rate of adsorbent materials packed in an adsorber bed. Two heat exchangers with different heat transfer surface area and fin spacing were packed with FAM-ZO2 and placed in an adsorber bed to study their performances under different cycle times. The results showed under a constant cycle time the adsorber bed in Design II provided higher uptake rate than that in Design I. Also, the adsorber bed in Design II could adsorb/desorb under shorter cycle times (8-20 min). The results also showed that the adsorber bed in Design II provided an SCP of 110 W/kg at cycle time of 8 min. Moreover, the SCP achieved using Design II was three times higher than that using Design I under cycle time of 60 min.

## Acknowledgement

The authors gratefully acknowledge the financial support of the Natural Sciences and Engineering Research Council of Canada (NSERC) through the Automotive Partnership Canada Grant No. APCPJ 401826-10.

## Nomenclature

$A$	heat transfer surface area ( $m^2$ )
$c$	heat capacity of solid materials ( $J/kg.K$ )
$c_p$	heat capacity at constant pressure ( $J/kg.K$ )
COP	coefficient of performance
$h_{fg}$	enthalpy of evaporation ( $J/kg$ )
$m$	mass ( $kg$ )
$\dot{m}$	mass flow rate ( $kg/s$ )
$P$	Pressure ( $kPa$ )
$Q_{total}$	total heat transfer ( $J$ )
SCP	specific cooling power ( $W/kg$ dry adsorbent)
$\omega$	adsorbate uptake ( $kg/kg$ dry adsorbent)
$T$	temperature ( $K$ )
$t$	time ( $s$ )
$\tau_{cycle}$	cycle time ( $s$ )

### Subscripts

adsorbate	adsorbate
adsorbent	adsorbent particles
cf	cooling fluid
cond	condenser
evap	evaporator
hf	heating fluid
$i$	in
$o$	out

## References

1. Buzelin L.O.S., Amico S.C., Vargas J.V.C., Parise J.A.R. Experimental development of an intelligent refrigeration system // *Int J Refrig.* 2005. Vol. 28. Pp. 165–75.
2. Farrington R., Rugh J. Impact of vehicle air-conditioning on fuel economy, tailpipe emissions, and electric vehicle range // *Proceeding Earth Technol. Forum*, Washington, D.C. 2000.

3. Suzuki M. Application of adsorption cooling systems to automobiles // *Heat Recover Syst CHP*. 1993. Vol. 13. Pp. 335–40.
4. Abdullah M.O., Tan I.A.W., Lim L.S. Automobile adsorption air-conditioning system using oil palm biomass-based activated carbon: A review // *Renew Sustain Energy Rev*. 2011. Vol. 15. Pp. 2061–72.
5. Demir H., Mobedi M., Ülkü S. A review on adsorption heat pump: Problems and solutions // *Renew Sustain Energy Rev*. 2008. Vol. 12. Pp. 2381–403.
6. Poyelle F., Guilleminot J.J., Meunier F. Experimental tests and predictive model of an adsorptive air conditioning unit // *Ind Eng Chem Res*. 1999. Vol. 38. Pp. 298–309.
7. Tamainot-Telto Z., Critoph R.E. Monolithic carbon for sorption refrigeration and heat pump applications // *Appl Therm Eng*. 2001. Vol. 21. Pp. 37–52.
8. Freni A., Tokarev M.M., Restuccia G., Okunev A.G., Aristov Y.I. Thermal conductivity of selective water sorbents under the working conditions of a sorption chiller // *Appl Therm Eng*. 2002. Vol. 22. Pp. 1631–42.
9. Sharafian A., Bahrami M. Adsorbate uptake and mass diffusivity of working pairs in adsorption cooling systems // *Int J Heat Mass Transf*. 2013. Vol. 59. Pp. 262–71.
10. Askalany A.A., Salem M., Ismael I.M., Ali A.H.H., Morsy M.G., Saha B.B. An overview on adsorption pairs for cooling // *Renew Sustain Energy Rev*. 2013. Vol. 19. Pp. 565–72.
11. Aristov Y. Concept of adsorbent optimal for adsorptive cooling/heating // *Appl Therm Eng*. 2014. Vol. 72. Pp. 166–75.
12. Himooka S.S., Shima K.O. The evaluation of direct cooling and heating desiccant device coated with FAM // *J Chem Eng Japan*. 2007. Vol. 40. Pp. 1330–4.
13. Henninger S.K., Schmidt F.P., Henning H.M. Water adsorption characteristics of novel materials for heat transformation applications // *Appl Therm Eng*. 2010. Vol. 30. Pp. 1692–702.
14. Dawoud B. On the Effect of Grain Size on the Kinetics of Water Vapor Adsorption and Desorption into/from Loose Pellets of FAM-ZO2 under a Typical Operating Condition of Adsorption Heat Pumps // *J Chem Eng Japan*. 2007. Vol. 40. Pp. 1298–306.
15. Sharafian A., McCague C., Bahrami M. Impact of fin spacing on temperature distribution in adsorption cooling system for vehicle A/C applications // *Int J Refrig*. 2015. Vol. 51. Pp. 135–43.